International Journal of Greenhouse Gas Control 85 (2019) 156–165

Contents lists available at ScienceDirect

International Journal of Greenhouse Gas Control

journal homepage: www.elsevier.com/locate/ijggc

# Enhancing $CO_2$ absorption for post-combustion carbon capture via zinc-based biomimetic catalysts in industrially relevant amine solutions

Leland R. Widger[a], Moushumi Sarma[a], Rachael A. Kelsey[a], Chad Risko[a,b], Cameron A. Lippert[a], Sean R. Parkin[b], Kunlei Liu[a,c,*]

[a] Center for Applied Energy Research, University of Kentucky, Lexington, KY, 40511, United States
[b] Department of Chemistry, University of Kentucky, Lexington, KY, 40506, United States
[c] Department of Mechanical Engineering, University of Kentucky, Lexington, KY, 40506, United States

ARTICLE INFO

*Keywords:*
Post-combustion
$CO_2$ capture
Mass transfer
Amine
Catalyst
Additives

ABSTRACT

Anthropogenic greenhouse gas emissions, such as $CO_2$ from fossil fuel combustion, are a global environmental, health, and economic concern. Aqueous amine-based $CO_2$ capture processes offer a technologically mature and relevant approach to $CO_2$ sequestration, although cost reduction strategies are still necessary for widespread deployment. Inspired by the metalloenzyme carbonic anhydrase (CA), we report the design, synthesis, and activity testing of zinc(II) complexes $[Zn^{II}(PSA^{AMP})Cl_2]$ (**1**) and $[Zn^{II}(PSA^{MEA})Cl_2]$ (**2**) as $CO_2$ hydration catalysts in aqueous amine solutions. The novel multifunctional ligand environment includes features in the primary and secondary coordination spheres that result in enhanced $CO_2$ mass transfer in industrially relevant carbon capture solvents and stability towards harsh industrial process conditions. Complexes that lack these key features do not show enhanced $CO_2$ absorption. Density functional theory (DFT) calculations that assess the catalytic pathway demonstrate how **1** and **2** catalyze $CO_2$ hydration analogous to CA. These catalysts increase mass transfer by 20–55% in lab scale experiments, offering the potential to reduce the cost of amine-based $CO_2$ capture processes without significantly altering industrial-scale system design, making rapid deployment of this critical bridge technology a viable strategy to reduce global greenhouse gas emissions.

## 1. Introduction

Concern over anthropogenic greenhouse gas emissions, such as $CO_2$ from fossil fuel combustion, is leading to new regulations on fossil-fuel fired power generation facilities, and unparalleled international agreements such as the Kyoto Protocol and the Paris Accords (Kyoto Protocol to the United Nations Framework Convention on Climate Change, 1998; Paris Agreement, 2016). Though critical to overall success, recent studies conclude that the 2050 emission reduction target associated with the long-term climate change goal of the Paris Agreement requires an unprecedented deployment of carbon capture and sequestration (CCS) technologies (Rogelj et al., 2016). Amine-based CCS systems are currently employed in a variety of industrial applications, including natural gas sweetening and acid gas cleanup for the cement and steel industries. As the most widely studied CCS technology, amine-based CCS is the most likely to be quickly implemented at full commercial scale for power generation applications. The long-standing record, known regulatory requirements, and deployment systems for this technology are attractive to the power generation industry that must weather a continually unstable economic and regulatory environment. However, full scale implementation of current carbon capture systems is estimated to increase the overall cost of electricity by 85% ($66/ton $CO_2$ captured) over a twenty-year levelized cost (Ciferno et al., 2009), and significant cost reduction strategies are critical to make widespread deployment economically viable (Desideri and Corbelli, 1998; Rao et al., 2002; Carbon Sequestration: Research and Development, 1999; Parson and Keith, 1998).

Increasing the mass transfer of $CO_2$ in the absorber can significantly reduce the cost of CCS by decreasing the sensible heat requirement and/or reducing the size of the absorber. There are two main factors in mass transfer, the reaction resistance and the liquid side diffusion resistance. (Mannel et al., 2017) One strategy to reduce reaction resistance has focused on the development of synthetic catalysts to increase the kinetics of the $CO_2$ hydration reaction (Floyd et al., 2013; Koziol et al., 2012; Zhang and Vaneldik, 1995; Zhang et al., 1993; Nakata et al., 2002; Huang et al., 2011a, b; Parkin, 2004) in slow hindered and tertiary amine solvents, or in the bottom section of the absorber for kinetically fast primary and secondary amines (Eq. (1)), where absorption

* Corresponding author.
*E-mail address:* Kunlei.Liu@uky.edu (K. Liu).

https://doi.org/10.1016/j.ijggc.2019.04.002
Received 20 August 2018; Received in revised form 21 March 2019; Accepted 3 April 2019

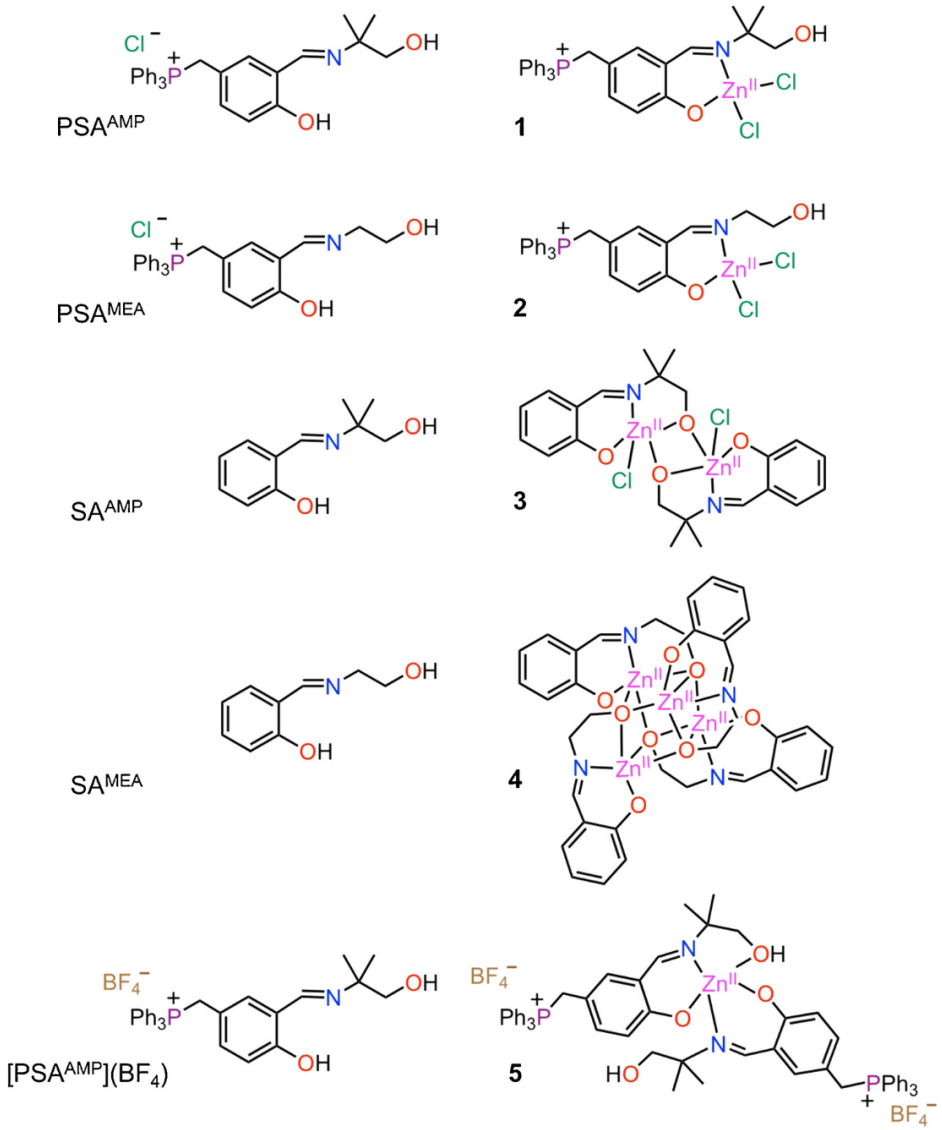


**Fig. 1.** Ligands (left) and corresponding complexes (right) discussed in this study. Select heavy atoms and chemical groups are highlighted in each compound.

slows with decreasing concentration of free amine and$CO_2$ hydration (Eq. (2) becomes more kinetically relevant.

$$2\ R\text{-}NH_2 + CO_2 \underset{}{\overset{\text{Fast}}{\rightleftharpoons}} R\text{-}NH\text{-}C(=O)\text{-}O^- \ H_3N^+\text{-}R \quad (1)$$

$$H_2O + CO_2 \underset{\text{pH ~9.5}}{\overset{\text{Slow}}{\rightleftharpoons}} HCO_3^- + H^+ \quad (2)$$

In biological systems, $CO_2$ hydration is catalyzed by the carbonic anhydrase (CA) family of metalloenzymes. The most widely studied CA contain a catalytically active Zn(II) center, which in the resting state is bound in a tetrahedral geometry by three histidine residues and an axial water. (Lindskog, 1997) The use of earth-abundant and non-toxic Zn, along with the fact that CA has some of the fastest known reaction rates of any catalyst ($K_{cat}$ ~ $10^6$ $M^{-1}s^{-1}$), make Zn-based biomimetic catalysts ideal candidates for the large scales required in CCS. The CA mimic $(Zn(cyclen)(H_2O))[ClO_4]_2$ has been widely studied as a potential $CO_2$ hydration catalyst for CCS, (Zhang and Vaneldik, 1995; Zhang et al., 1993; Nakata et al., 2002; Huang et al., 2011a; Davy, 2009;), however the Zn center is electronically unsaturated and shows high levels of product inhibition from bicarbonate anion coordination, leading to low catalyst activity under industrially relevant conditions (Floyd et al., 2013). The majority of early CA mimics were only evaluated under dilute stopped-flow conditions in kinetically slow tertiary amine or carbonate solvents, and were not able to approach the capture rates of kinetically fast primary amine solvents. These early studies (Floyd et al., 2013; Lau et al., 2013; Koziol et al., 2013) identified presumed guidelines for further catalyst development: (i) tetradentate ligands are required to chelate the metal ion within the ligand environment and prevent demetallation in amine solvents; (ii) similar to the native enzyme, Zn(II) is more active than Co(III) due to increased Lewis acidity; and (iii) bicarbonate inhibition of the catalyst will likely occur, especially in hindered or tertiary amine solvents. It, therefore, becomes apparent that small molecule catalysts need to incorporate biomimetic secondary coordination sphere components analogous to those in the CA enzyme, such as a hydrophobic binding pocket and a hydrogen bond donor (Koziol et al., 2013).

Secondary coordination sphere effects, such as hydrogen bonding interactions and local polar/non-polar pockets, have long been understood to be critical components to the activity and specificity of many

metalloenzymes and transition metal complexes, and are still widely under investigation today. (Shook and Borovik, 2010a; Span et al., 2017) Despite their importance, careful examination of secondary coordination sphere interactions has only recently garnered increased attention in biomimetic inorganic model complexes, with most effort still focused on replicating the immediate coordination environment of the metal center. Hydrogen-bonding groups have been incorporated into some biomimetic M-$O_x$ motifs, (Lacy et al., 2013; Shook and Borovik, 2010b; Gupta et al., 2012; Berreau et al., 2001; Soo et al., 2009; Kim et al., 2012; Sahu et al., 2013, 2014; Sahu et al., 2016; Widger et al., 2014a, b; Wada et al., 1998) with these interactions generally stabilizing adducts, including a Ni-bicarbonate complex derived from $CO_2$ hydration. (Guillet et al., 2015) Notably, these studies are usually carried out in pure organic solvents, which are far from the aqueous amine solutions used in commercially relevant CCS systems. In contrast, hydrogen bonding from Lysine48 (Lys48) in superoxide reductase is responsible for favoring proper M—O bond cleavage over O—O bond cleavage that predominates in the Lys48 knockout (Bonnot et al., 2012). This type of destabilizing interaction of the M—O bond, seen at a solvent-exposed active site in an aqueous environment, would be favorable for catalytic turnover in biomimetic CAs, where slow bicarbonate dissociation remains an issue.

Previous work from our lab has described the first examples of biomimetic $CO_2$ hydration catalysts to increase $CO_2$ absorption in amine based solvents under industrially relevant conditions. (Lippert et al., 2014a, b) The efficacy of these catalysts undermines conventional wisdom in the field (*vide supra*), where a Co(III)-containing catalyst demonstrated good enhancement activity and a bidentate Zn(II) complex was stable in CCS conditions. (Lippert et al., 2014a) The knowledge that the bidentate Zn(II) complex is just as effective as chelating tetradentate complexes allows for further development of complexes with bidentate ligand structures and labile ancillary ligands, as well as opening the possibility for incorporating additional functionalization in the secondary coordination sphere while maintaining a facile and scalable synthesis for industrial applications. Here we expand on these initial efforts through the design and synthesis of a new series of zinc(II) complexes (Fig. 1), and their characterization as $CO_2$ hydration catalysts in aqueous amine solutions. The multifunctional ligand environments of these complexes result in enhanced (i) $CO_2$ mass transfer (by 20–55% in lab scale experiments) in industrially relevant carbon capture solvents and (ii) stability towards harsh industrial process conditions. We also carry out density functional theory (DFT) calculations to propose the catalytic pathway followed by these complexes, which demonstrate that **1** and **2** behave analogously to CA for $CO_2$ hydration. Importantly, the catalyst design paradigm discussed here offers the potential to reduce the cost of amine-based $CO_2$ capture processes without significantly altering industrial-scale systems, enabling rapid deployment of bridge technologies to reduce global greenhouse gas emissions.

## 2. Experimental

### 2.1. Synthesis of 1 – 5

In producing a catalyst for large scale commercial applications, such as post-combustion carbon capture, ease of synthesis/purification and cost of production are critical components. The complexes **1 – 5** are all synthesized in a maximum of four synthetic steps (see supplementary material), where the pure desired product is a precipitate that is collected by filtration, without the need for any further work-up.

### 2.2. pH drop method

(Kelsey et al., 2016; Bond et al., 2001) In a representative procedure, the pH-drop solvent evaluation apparatus consists of a 30 ml gas water saturator, one mass flow controller, one glass impinger, one pH probe and a two-necked round-bottom flask that contains 50 mL of testing solution consisting of 30% aqueous MEA in the presence of **1** (2.0 mmol). Both saturator and impinger are made of Pyrex®. A simulated flue gas containing 14% $CO_2$ in $N_2$ span stream is saturated with water (15 mL) in the saturator and bubbled through the testing solvent in the round bottom flask through the impinger. One pH-probe is placed in the solution through the other neck of the round-bottom flask to measure the change in pH with time. A mass flow controller was installed to get a constant gas flow throughout the process. The gas flow was maintained at 0.6 L/min. The change of pH was monitored with time as the simulated flue gas was bubbled through the capture solution.

### 2.3. Breakthrough solvent evaluation method

(Lippert et al., 2014a; Kelsey et al., 2016) The breakthrough solvent evaluation apparatus consists of a 30 ml gas saturator, a bubbler that contains 50 mL of solution, two condensers, and a $CO_2$ analyzer. Both saturator and bubbler are made of Pyrex®, and are immersed in a water bath maintained at testing temperature. $CO_2$ feed gas stream balanced with $N_2$ is saturated with water in the saturator and bubbled through the testing solvent in the bubbler. The gas effluent is dried and analyzed for $CO_2$ concentration using a $CO_2$ analyzer (VIA-510, HORIBA, 0.5% precision). Data of $CO_2$ outlet concentration with respect to time is continuously recorded with 1 s interval using an in-house Labview program.

The difference -between inlet and outlet $CO_2$ concentration represent the absorbed amount of $CO_2$ at a particular time. The integration of the concentration difference represents the $CO_2$ loading as expressed in (Eq. (3))

$$\text{CO}_2\ \text{Loading (mol CO}_2\text{/kg solution)} = \frac{\int_0^t (C_{in} - C_{out}(t))dt}{m_{sol}} \quad (3)$$

in which $C_{in}$ is the $CO_2$ feed gas rate in mol/s, $C_{out}$ is the $CO_2$ effluent rate in mol/s, $t$ is time in second, and $m_{sol}$ is the mass of solution in kg.

In addition, the absorption rate can be described by the derivate of $CO_2$ loading with respect to time (Eq. (4)):

$$\text{Absorption rate (mol CO}_2\text{/kg solution/s)} = \frac{d\ \text{CO}_2\ \text{Loading}}{dt} \quad (4)$$

### 2.4. Evaluation of $NO_x$ and $SO_x$ stability

In a representative procedure, stock solutions of complex **1** (0.573 g, 3.8 mM, 250 mL) were prepared in 30 wt.% aqueous MEA. A 25 mL aliquot of the stock solution was treated with 1000 ppm $NaNO_2$ (0.250 g of $NaNO_2$) for 24 h followed by evaluation in the pH-drop apparatus for the above method. This method was repeated for treatments with 1000 ppm $NaNO_3$, $Na_2SO_4$, and the combination of the three for a total concentration of 3000 ppm $NO_x$ and $SO_x$ derived salts. Gaseous $NO_x$ contaminants were generated in-situ and bubbled through a 25 mL aliquot of the stock solution containing 4 mM of complex **2** for 30 min prior to evaluation via the pH-drop apparatus. For the generation of $NO_x$ gas, a 100 mL two-necked round bottom flask was charged with solid $NaNO_2$ (2.25 g, 0.033 mol) and a magnetic stir bar. One neck was sealed with a rubber septum, and the other was fitted with a glass adapter containing a hose barb. Rubber tubing was attached via the hose barb adapter and a needle was fitted to the end of the rubber tubing. Concentrated sulfuric acid was added dropwise through the septum with constant stirring resulting in the immediate appearance of a brown fume.

### 2.5. Evaluation of catalyst thermal stability

In a representative procedure, a stock solution of complex **1** (3.8 mM) was prepared in a 30 wt.% aqueous MEA solution. A 50 ml aliquot was taken from the stock solution and 14% $CO_2$ gas with $N_2$ span was bubbled through the solution until a pH of 10.5 was reached. The solution was transferred to an autoclave, sealed, placed in an oven, and heated at 145 °C for 92 h at which point the autoclave was removed from the oven and cooled to room temperature. The activity of the catalyst was assayed by taking a 25 mL aliquot and evaluating via the pH-drop method as described above.

### 2.6. DFT calculations

All density functional theory (DFT) calculations were carried out using the M06 functional (Zhao and Truhlar, 2008) in conjunction with the cc-pvdz basis set (Dunning, 1989). To account in part for the aqueous environment in which the catalytic reactions take place, the solvation model based on density (SMD) was implemented, and the solvent option was chosen to be water (ε = 78.3553) (Scalmani and Frisch, 2010). Normal mode analyses were performed for all optimized structures to ensure that the geometries represent energetic minima. All calculations were carried out with the Gaussian09 (Revision A.02) software suite (Frisch et al., 2009). We note that the systems under investigation possess a wide degree of conformational variability, given the flexibility of the ligands. It is expected that this conformational variability will be extensively explored in solution under operational conditions. Assorted conformations, in particular with respect to the hydrogen bond donor arm, were surveyed during the initial optimization of the neutral, unreacted species. The low energy structures from these tests were then used as the bases for the follow-up catalytic reaction path explorations.

## 3. Results & discussion

### 3.1. Catalyst design and function

To obtain the features of CA without the large complex enzyme structure, the $PSA^{alkanolimine}$ ligand scaffold, based on 5-(triphenylphosphoniummethyl)salicylaldehyde (PSA) with ethanolamine (MEA) or 2-amino-2-methyl-1-propanol (AMP) as the alkanolamine, was employed in the synthesis of $[Zn^{II}(PSA^{AMP})Cl_2]$ (**1**) and $[Zn^{II}(PSA^{MEA})Cl_2]$ (**2**) (Fig. 2). These complexes incorporate a triphenylphosphonium moiety on the ligand backbone and a hydrogen bond donor arm that is positioned to form a biomimetic pocket around the catalytically-active metal ($Zn^{II}$) center. In addition, the cationic triphenylphosphonium moiety on the ligand backbone provides additional charge that is balanced by the phenoxide on the ligand and the two ancillary chloride ligands coordinated to the $Zn^{II}$ center. The analogous complexes $[Zn^{II}(SA^{AMP})Cl]_2$ (**3**) and $[Zn^{II}(SA^{MEA})]_4$ (**4**) were synthesized from the $SA^{alkanolimine}$ ligand scaffold, based on salicylaldehyde (SA), which lacks the triphenylphosphonium moiety (Fig. 1). Without the additional charged triphenylphosphonium backbone the $Zn^{II}$ centers in complexes **3** and **4** are coordinatively unsaturated, forming a dimer and tetramer in the solid state (see supplementary material for crystallographic details). Complex **5** ($[Zn^{II}(PSA^{AMP})_2](BF_4)_2$), where the triphenylphosphonium moiety is present on the ligand backbone but the ancillary chloride ligands are replaced with non-coordinating tetrafluoroborate ($BF_4$-) counterions, was synthesized for comparative reactivity studies. In the absence of a coordinating anion to electronically and coordinatively saturate the $Zn^{II}$ center, complex **5** forms a *bis* complex where the Zn(II) center is bound in a trigonal bipyramid by two $PSA^{AMP}$ ligands, with the two anionic phenoxide donors, two imine N-donors and one of the hydrogen bonding alcohol groups in the axial position. The positive charge from the cationic backbone moieties is balanced by the two non-coordinating $BF_4$– counterions. These structural differences observed in the crystallography will have considerable impact on the performance of these complexes in $CO_2$ hydration (*vide infra*).

The Zn(II) complexes **1 – 5** were initially screened for their ability to increase mass transfer of $CO_2$ in industrially relevant amine-based CCS solvents by the pH drop method (30% MEA, Fig. 3; 15% DEA and 0.3 M MDEA, see supplementary material). (Kelsey et al., 2016) Complexes **1** and **2** show enhancement in the overall $CO_2$ removal rate for the three solvents tested, while no enhancement is observed when the metal salt ($ZnCl_2$) is added without the $PSA^{alkanolamine}$ ligand. (Lippert et al., 2014a) The addition of **1** has a negligible effect on the solvent physical properties (see supplementary material), suggesting that the enhancement observed in the pH drop method is the result of the catalytic activities of these complexes, and not of Zn(II) ions from complex degradation or physical changes in the solvent that occur upon catalyst addition.

In contrast to **1** and **2**, complexes **3 – 5** are all inactive in primary amine solution (Fig. 3), providing insight into the structural factors that influence the activity of these complexes toward $CO_2$ capture reactions. While the X-ray structures of **1** and **2** (Fig. 2) show well defined mononuclear complexes with two *cis*- labile ligands at the metal binding sites, **3** is a dinuclear complex, **4** is a tetramer, and **5** forms a *bis* complex. Steric factors on the alkanolamine ligand arm are likely the cause of differences in oligomerization of **3** and **4**, while replacing the ancillary chloride ligands with non-coordinating $BF_4$– counter ions in **5** leaves the $Zn^{II}$ center coordinatively unsaturated and leads to the formation of a *bis* complex with an additional ligand equivalent. The AMP methyl groups in **3** prevent the formation of larger order structures as in **4**. This structural change from mononuclear to oligomers is likely due to the lack of the cationic triphenylphosphonium moiety on the backbone, where an additional anion is no longer required to balance the charge. Complex **3** does retain one ancillary chloride ligand bound to the $Zn^{II}$ center while **4** is electronically and coordinately saturated by ligand donors. The larger and less polar structures render **3** and **4** less soluble in aqueous amine solvents and the structures do not show the presence of any sort of binding pocket to facilitate $CO_2$ binding or bicarbonate dissociation. We hypothesize that the structure of the binding pocket in

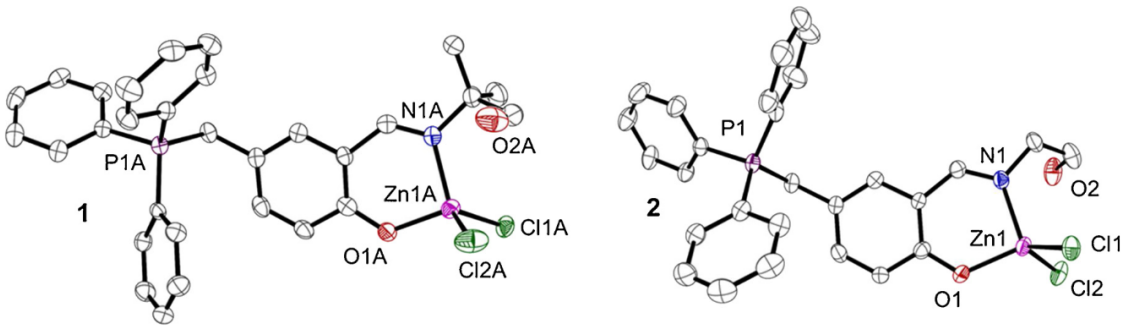


**Fig. 2.** Displacement ellipsoid plots for **1** and **2** (50% probability level). H atoms are removed for clarity.

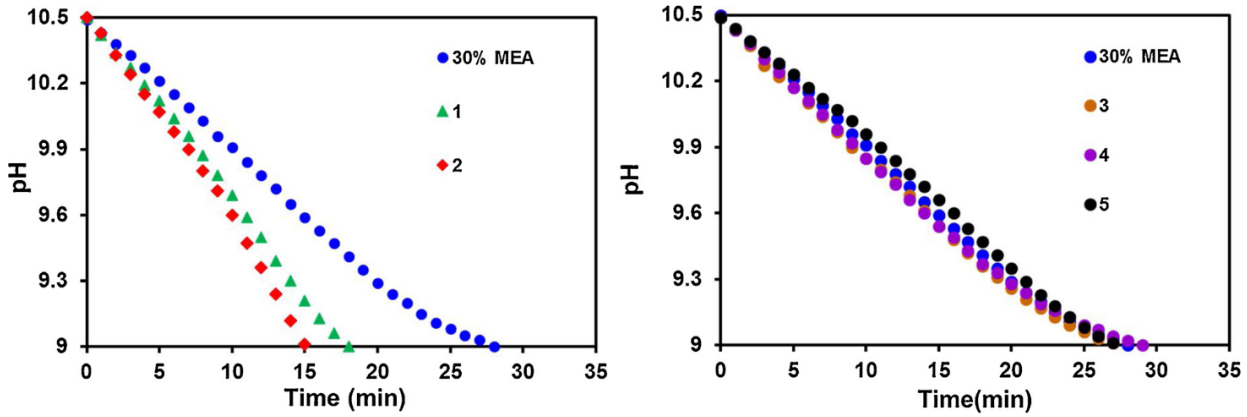


**Fig. 3.** pH Drop testing of complexes **1** – **5** in 30% MEA.

**1** and **2**, as shown by the following DFT calculations, is an important feature for catalyst activity under CCS conditions. This is reminiscent of the native CA enzyme where site directed mutagenesis studies reveal that even minor modifications of the wild-type active site "pocket" can have significant deleterious effects on catalytic efficiency, and larger substitutions render the enzyme essentially dead. (Domsic and McKenna, 2010; Alexander et al., 1991) The catalytic pocket directs $CO_2$ approach for binding and facilitates reaction with zinc-bound hydroxide to produce bicarbonate, as well as subsequent product dissociation, mimicking the amphiphilic pocket in wild-type CA.

While pH drop is an effective method for rapid initial screening of catalyst candidates, quantitative $CO_2$ removal rate data was obtained via breakthrough experiments where simulated flue gas (14% $CO_2/N_2$) is bubbled through the amine solution until it is saturated. Monitoring of the $CO_2$ concentration at the outlet allows for the calculation of the $CO_2$ removal rate as a function of carbon loading. The extensive mixing in the breakthrough apparatus minimizes the diffusion resistance and allows for the observation of changes in the reaction side resistance to mass transfer ($K_G$), (Mannel et al., 2017; Widger et al., 2017) within the concentrated industrially-relevant solvents that preclude the use of other fundamental characterization techniques (e.g. UV–vis, etc). With all other variables held constant, the data in Fig. 4 show a 15–40% increase in the rate of $CO_2$ removal at all carbon loading values for solutions of 30% MEA containing **1** (3.8 mM) and **2** (4 mM). Catalysts **1** and **2** are also active in the representative secondary and tertiary amine solvents, 15% DEA (diethanolamine, Fig. 4) and 0.3 M MDEA (methyldiethylamine, see supplementary material) respectively, indicating these catalysts can be utilized in kinetically slower solvents to increase mass transfer as well as in fast solvents such as MEA. Catalytic enhancement by **1** and **2** in a tertiary amine solvent, where the amine does not react with $CO_2$ directly, indicates that the enhancement is from the direct reaction of $CO_2$ with the catalytic complexes, similar to the proposed mechanism for $CO_2$ hydration by CA. This is further supported by the percent enhancement plots (Fig. 4) that show the degree of enhancement increases (relative to the baseline) for all solvents at higher loadings ($> \alpha$ 0.3), where the concentration of free amine decreases and the kinetics become increasingly dominated by the slow $CO_2$ hydration reaction. Increasing the $CO_2$ absorption rate at higher loadings is the primary goal for developing $CO_2$ hydration catalysts. Incremental increases in absorption kinetics within this region can decrease the required absorber height and save on capital costs for construction. Achieving a richer solvent loading within an existing absorber can also save on operational costs by allowing for decreased liquid circulation rates and decreased sensible heat requirement for regeneration.

### 3.2. Density functional theory

Due to the complex nature of aqueous amine-containing CCS solvents, detailed fundamental and spectroscopic studies are difficult. To probe elementary relationships among catalyst structure and mechanism, DFT calculations at the SMD/M06/cc-pvdz level of theory were undertaken. The di-chloride bound resting state for **1** sugggests that in solution the triphenylphosphonium group is folded toward the Zn(II) center forming a hydrophobic binding pocket around the metal center. Further, the alcohol −OH is directed toward the axial chloride ligand (O—H···Cl distance of 2.28–2.30 Å); this conformation is favored over O—H···Cl interaction with the equatorial chloride by ~4 kcal/mol. While there is essentially no difference between dissociation of the two chloride ligands for water binding to the Zn(II) center, the axial position (within the pocket) is preferred for deprotonation of Zn—$OH_2$ and formation the Zn—OH species, where the alcohol—OH is hydrogen bonded to the Zn—OH (O–H···OH–Zn distance of 1.69 Å; Fig. 5). Analysis of the highest-occupied molecular orbital (HOMO) of Zn − OH shows the wavefunction extending onto the Zn-bound hydroxyl group, suggesting a high nucleophilicity for $CO_2$ hydration.

For the association of $CO_2$, the energetic approach to the Zn-bound −OH and subsequent binding is downhill. Proton transfer produces the Lipscomb binding orientation of the bicarbonate product, a species that is energetically stabilized compared to the $CO_2$-associated system (previous step), and the alcohol OH remains directed toward the ligand. The key bicarbonate dissociation step, which is rate determining in synthetic systems, occurs when $[HCO_3]-$ dissociates and $H_2O$ rebinds to reactivate the catalyst. The energy to dissociate $[HCO_3]-$ from the catalyst is ~32 kcal/mol from the axial position (within the pocket), and ~24 kcal/mol from the equatorial position (outside the pocket). Overall, the reaction taking place within the pocket is generally more energetically preferred throughout the catalytic cycle, and allows for a slightly less facile dissociation of the $[HCO_3]-$ due to the secondary coordination effects.

Although there are reports of strategies to increase $CO_2$ absorption, including $CO_2$ hydration catalysts for kinetically slow solvents such as tertiary amines, (Liang et al., 2015; Sivanesan et al., 2017) there are limited reports of homogeneous catalysts that show enhancement of $CO_2$ removal in kinetically fast primary amine solvents that are the most likely to be implemented commercially. (Lippert et al., 2014a, b; Kelsey et al., 2016) The complexes discussed here contain anionic ligands that donate electron density into the metal center, thereby facilitating bicarbonate/anion dissociation and increasing $CO_2$ hydration rates. The higher electron density of the catalyst core as well as the covalently attached cationic water solubilizing groups may serve to remove anionic bicarbonates/carbamates from the secondary coordination sphere and away from the metal center. We propose the above as key features in achieving catalytic rates large enough to contribute to the overall mass transfer in concentrated primary amine-based solvents, thereby increasing the rate of $CO_2$ absorption. The addition of the homogenous catalyst does not significantly alter the pH or

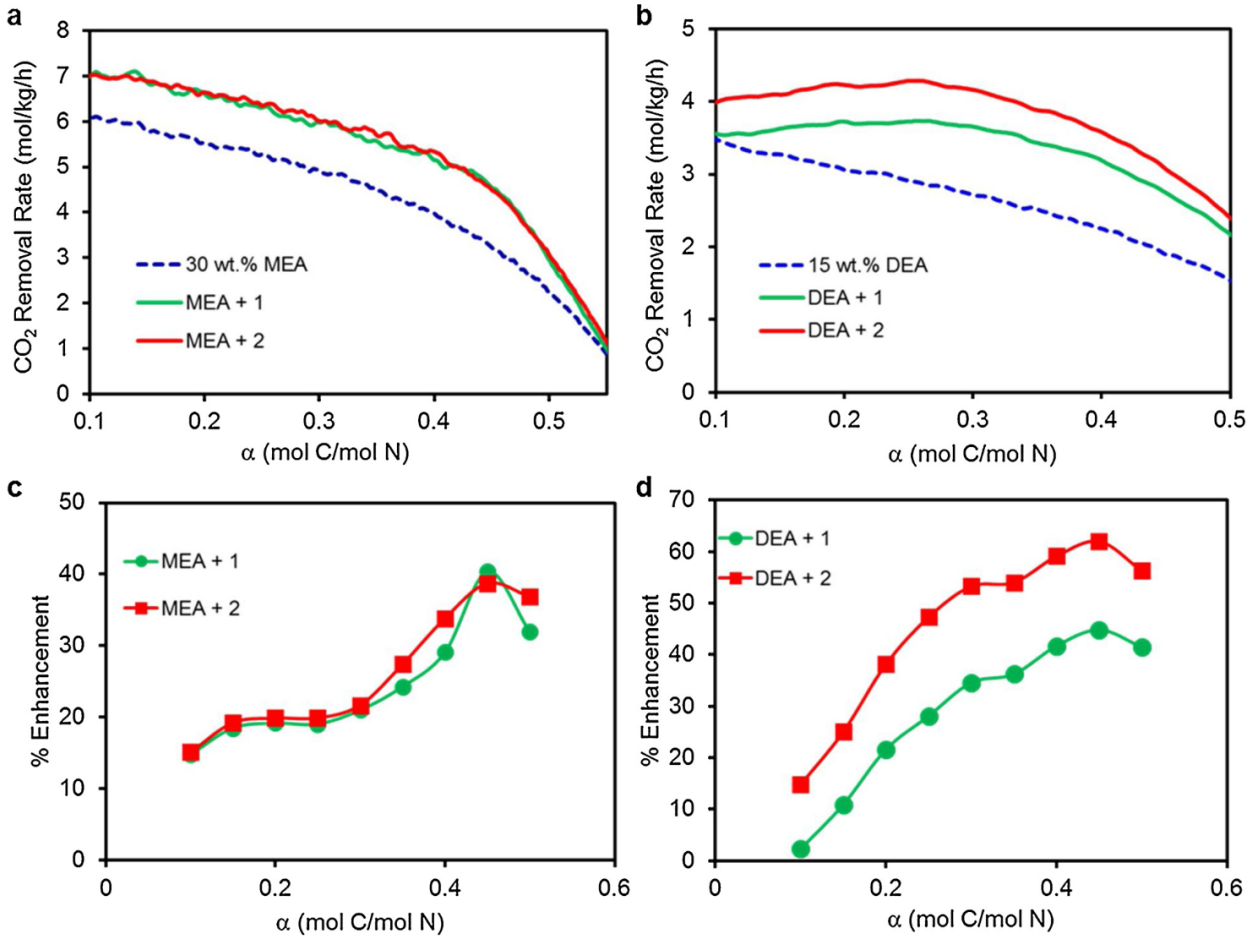


**Fig. 4.** Breakthrough studies for **1** and **2** in 30% MEA (**a**) and 15% DEA (**b**). Percent enhancement in $CO_2$ removal rate over the solvent baseline for solutions of 30% MEA (**c**) and 15% DEA (**d**) containing **1** and **2**.

physical properties of the amine solvents such as viscosity and surface tension (see supplementary material) that are well known to effect mass transfer. (Bryant et al., 2016; Gómez-Díaz et al., 2009) Although there is a slight decrease in surface tension (˜5 dyne/cm) for solutions of 30% MEA with **1**, this is insignificant compared to the ˜40 dyne/cm change observed upon the addition of a commercial surfactant that showed similar improvement. (Bryant et al., 2016) Therefore two possible mechanisms may explain the increased rate of absorption: 1) the catalysis of $CO_2$ hydration, and/or 2) the conversion of bicarbonate to carbamate in the presence of primary amines.

The enhancement and properties of **1** and **2** in the representative alkanolamine solvents MEA, DEA, and MDEA are broadly applicable to the majority of commercially viable amines that would be used in a CCS solvent. Most solvents that meet the cost, stability, reactivity, and regulatory/emissions requirements for a viable process are either slightly modified amines or alkanolamines, and have similar chemical and physical properties. Although there may be some differences in operation for primary, secondary, or tertiary amines, the underlying technology is the same and utilizes similar components and process conditions. It is therefore important to ensure **1** and **2** are stable to a representative set of these conditions.

### 3.3. Process stability

In industrial CCS processes, the amine solvent and any solvent additives are constantly exposed to a variety of harsh conditions. Temperatures in the stripper reach 120 °C or higher, making amine degradation and subsequent make-up a key area of added operational costs. In addition, coal-derived flue gas inherently has a variety of contaminants that are not necessarily present in other applications, such as natural gas combustion. While the widespread use of flue gas desulfurization (FGD) has significantly reduced some of these contaminants, there are still considerable levels of oxidizing $NO_x$ and $SO_x$ that are concentrated in the solvent loop. (Huang et al., 2014; Chandan et al., 2014) It is therefore critical to ensure that any process additives are stable toward the high temperatures and oxidizing flue gas contaminants over extended periods. The stability of **1** and **2** was verified in a series of pH drop experiments where the activity of solutions containing **1** and **2** in 30% MEA were exposed to harsh thermal or oxidizing conditions and normalized to the additive free MEA baseline. The data in Fig. 6a shows no significant decrease in catalyst activity when solutions containing **1** and **2** are heated to 145 °C for up to 96 h. Although this is only a model for a heat-integrated process, we can estimate that 96 h of continual heating translates to at least 2 months of constant process operation, assuming 10% residence time in the stripper, during which no loss in activity is observed. In addition, Fig. 6b shows no decrease in relative activity of **1** and **2** upon the addition of 1000 ppm NOx and SOx, concentrations that are on the order of those observed in industrial CCS processes. (Thompson et al., 2014, 2017)

Amine-based CCS solvents at high $CO_2$ loadings ($\alpha > 0.40$ mol C/mol N) contain high concentrations of anions such as carbamates and bicarbonates. These species are known catalyst inhibitors and are typically the main cause of poor catalytic activity in previously reported

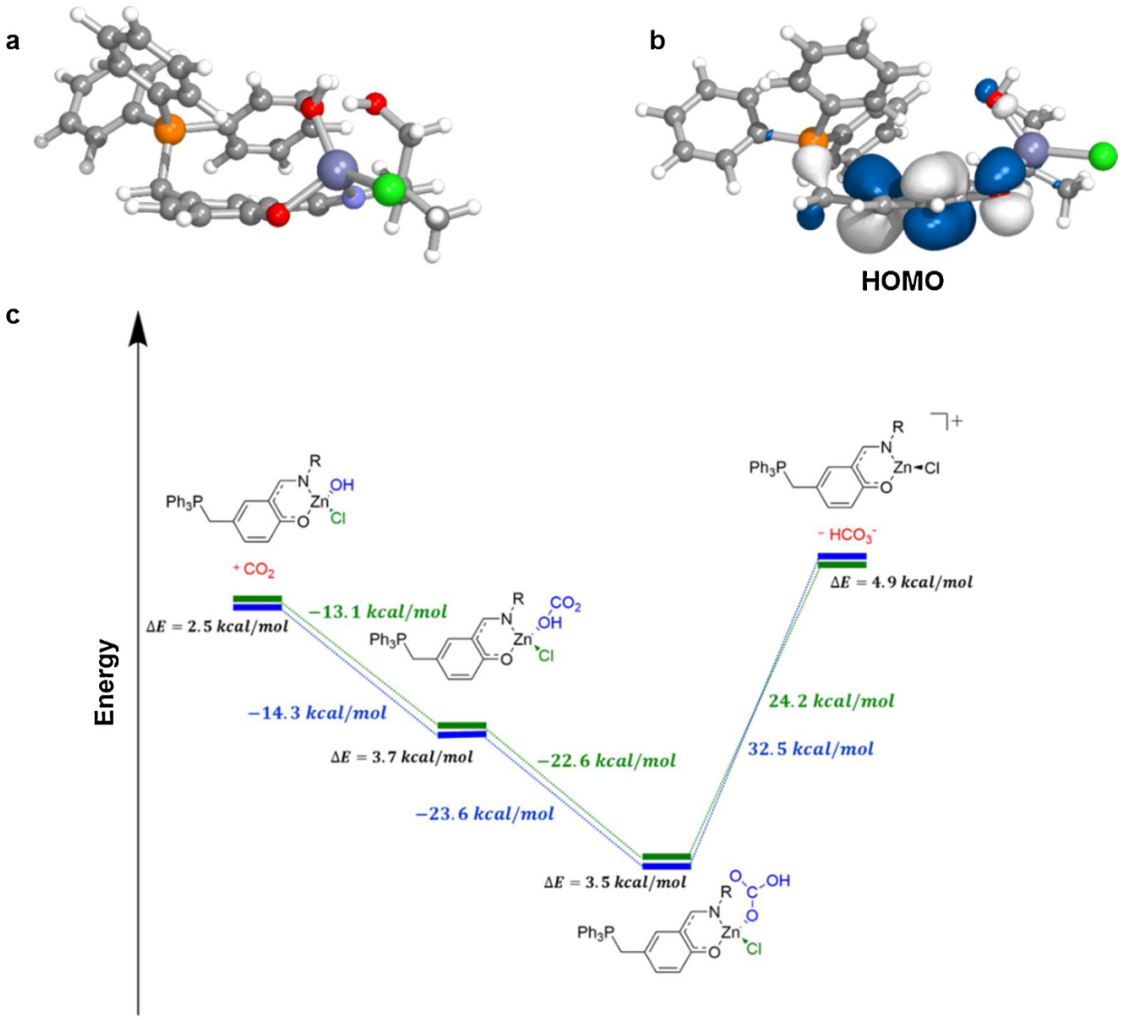


**Fig. 5.** a) Structure of the Zn–OH form of **1** that reveals the binding pocket and hydrogen bonded coordination, b) pictorial representation of the Zn–OH HOMO, and c) relative energies of catalytic $CO_2$ hydration at the axial (green) and equatorial (blue) labile sites as determined at the SMD-M06/cc-pvdz level of theory.

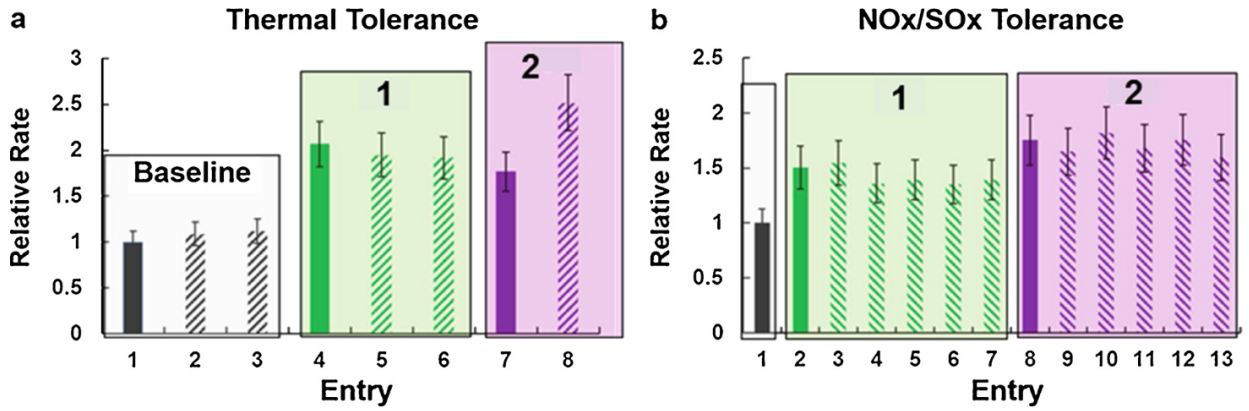


**Fig. 6.** Relative rates of $CO_2$ adsorption, normalized to 30% MEA, under **a**) thermal conditions and b) oxidizing conditions. Entries: a) 1. Baseline 30% MEA; 2. 30% MEA after 15 h exposure at 145 °C; 3. 30% MEA after 90 h exposure at 145 °C; 4. Addition of catalyst **1**; 5. Addition of **1** after 15 h exposure at 145 °C; 6. Addition of **1** after 90 h exposure at 145 °C; 7. Addition of **2**; and 9. Addition of **2** after 90 h exposure at 145 °C. Entries **b**) 1. Baseline 30% MEA; 2. Addition of **1**; 3. Addition of **1** and 1000 ppm nitrate, 4. Addition of **1** and 1000 ppm nitrite, 5. Addition of **1** and 1000 ppm sulfate; 6. Addition of **1** and *in-situ* generated NOx gas; 7. Addition of **1** and 1000 ppm nitrate, nitrite, and sulfate each; 8. Addition of **2**; 9. Addition of **2** and 1000 ppm nitrate; 10. Addition of **2** and 1000 ppm nitrite; 11. Addition of **2** and 1000 ppm sulfate; 12. Addition of **2** and 1000 ppm nitrate, nitrite, and sulfate each.

CA mimics. (Nakata et al., 2002; Lau et al., 2013) However (Zhang et al., 1993), C-NMR and UV–vis experiments show no change upon addition of excess bicarbonate to **1** and **2**, and neither pH drop or breakthrough experiments show any decrease in activity in the presence of bicarbonate (see supplementary material). The overall stability of **1** and **2** to all of these process factors is critical for sustained catalytic activity, resisting thermal and oxidative degradation, and stability at high carbon loadings is an indication that the ligand design is sufficient to disfavor degradation and bicarbonate inhibition.

## 4. Conclusions

The homogenous catalysts **1** and **2** are effective additives for increasing the mass transfer of $CO_2$ in common amine-based CCS solvents, including kinetically fast solvents such as MEA. In addition, **1** and **2** are stable toward the harsh industrially relevant conditions found in CCS systems. The structural analogs **3**, **4**, and **5**, which lack the amphiphilic moiety on the ligand backbone and the ancillary chloride ligands respectively, adopt dimer and tetramer structures and show no activity towards increasing mass transfer into CCS solutions. DFT calculations reveal how the formation of a bi-functional "pocket" around the labile site of the catalytic metal center is essential to the mechanism: The triphenylphosphonium aryl groups provide a hydrophobic environment for the delivery of $CO_2$ to the metal center, while the hydrogen bonding arm of the ligand is favorably positioned for Zn − OH stabilization and hydrogen-bonding to the bicarbonate product to facilitate dissociation. In addition, the cationic phosphonium acts as an additional electrostatic force to draw bicarbonate away from the zinc center, and the overall anionic ligand environment is believed to further facilitate catalytic turnover. (Kelsey et al., 2016) The data from both theory and experiment indicate that catalysts **1** and **2** are functioning as designed, to catalyze the $CO_2$ hydration reaction via a mechanism analogous to the native CA metalloenzyme (Fig. 7). The $PSA^{alkanolamine}$ ligand scaffold provides an excellent starting point for further rational tuning of this catalytic pocket in the extended coordination sphere. The next stage is bench and pilot scale testing of **1** and **2**, where previous studies have shown a significant decrease in the overall energy penalty of a heat-integrated absorption-desorption process by other $CO_2$ hydration catalysts. (Widger et al., 2017) The previous Co(III)-based catalyst showed only a 10% improvement in $CO_2$ removal rate (at $\alpha = 0.3$ mol C/mol N) in the breakthrough apparatus, and gave a > 20% overall decrease in energy penalty when examined in a heat-integrated absorption/desorption process. (Widger et al., 2017) The $CO_2$ removal rates with **1** and **2** are showing a 20% improvement in MEA and a 35–55% improvement in DEA with the breakthrough apparatus, which could translate to an even larger energy saving compared to previous catalysts.

## Competing financial interest

The authors declare no competing financial interest.

## Acknowledgments

We thank the Carbon Management Research Group (CMRG), and

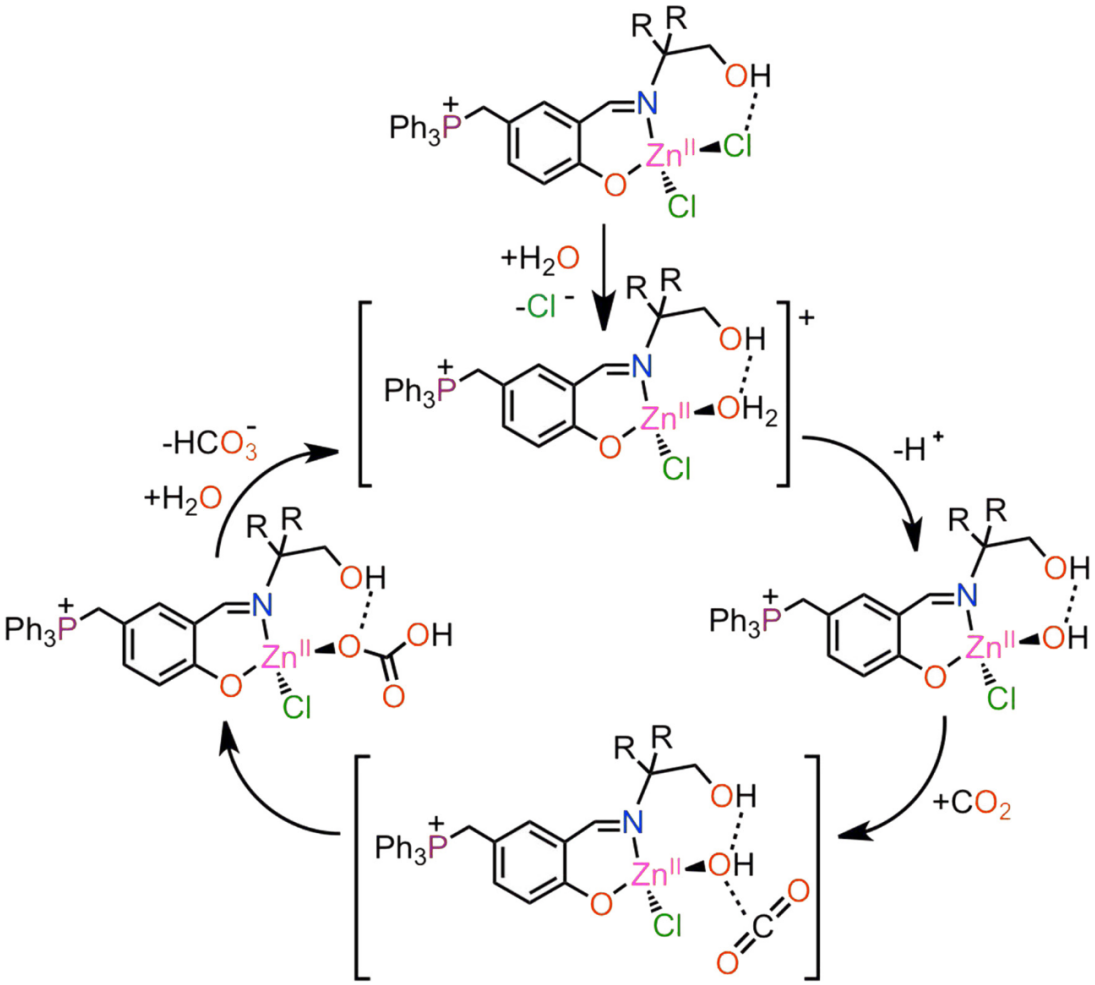


**Fig. 7.** Proposed catalytic cycle for $CO_2$ hydration by catalysts 1 (R = $CH_3$) and 2 (R = H).

US-China Clean Energy Research Center – Advanced Coal and Technology Collaboration (DE-PI0000017) for funding. C.R. thanks the University of Kentucky (UK) and UK Vice President for Research for start-up funds. Supercomputing resources on the Lipscomb High Performance Computing Cluster were provided by the UK Information Technology Department and Centre for Computational Sciences (CCS).

## Appendix A. Supplementary data

Supplementary material related to this article can be found, in the online version, at doi:https://doi.org/10.1016/j.ijggc.2019.04.002.

## References


Alexander, R.S., Nair, S.K., Christianson, D.W., 1991. Engineering the hydrophobic pocket of carbonic anhydrase II. Biochemistry 30 (46), 11064–11072.

Berreau, L.M., Makowska-Grzyska, M.M., Arif, A.M., 2001. Modeling the active site chemistry of liver alcohol dehydrogenase: mononuclear zinc methanol and N,N-dimethylformamide complexes of a nitrogen/sulfur ligand possessing an internal hydrogen bond donor. Inorg. Chem. 40 (10), 2212–2213.

Bond, G.M., Stringer, J., Brandvold, D.K., Simsek, F.A., Medina, M.G., Egeland, G., 2001. Development of integrated system for biomimetic CO2 sequestration using the enzyme carbonic anhydrase. Energy Fuels 15 (2), 309–316.

Bonnot, F., Molle, T., Menage, S., Moreau, Y., Duval, S., Favaudon, V., Houee-Levin, C., Niviere, V., 2012. Control of the evolution of iron peroxide intermediate in superoxide reductase from Desulfoarculus baarsii. Involvement of lysine 48 in protonation. J. Am. Chem. Soc. 134 (11), 5120–5130.

Bryant, J.J., Lippert, C., Qi, G., Liu, K., Mannel, D.S., Liu, K., 2016. Enhanced carbon capture through incorporation of surfactant additives. Ind. Eng. Chem. Res. 55 (27), 7456–7461.

Carbon Sequestration: Research and Development, 1999. A U.S. Department of Energy Report. Office of Science, Office of Fossil Energy, U.S. Department of Energy.

Chandan, P.A., Remias, J.E., Liu, K., 2014. Possible ways to minimize nitrosation reactions during post-combustion $CO_2$ capture process. Int. J. Greenhouse Gas Control 31, 61–66.

Ciferno, J.P., Fout, T.E., Jones, A.P., Murphy, J.T., 2009. Capturing carbon from existing coal-fired power plants. Chem. Eng. Prog April.

Davy, R., 2009. Development of catalysts for fast, energy efficient post combustion capture of $CO_2$ into water; an alternative to monoethanolamine (MEA) solvents. Energy Procedia 1 (1), 885–892.

Desideri, U., Corbelli, R., 1998. $CO_2$ capture in small size cogeneration plants: technical and economical considerations. Energy Convers. Manage. 39 (9), 857–867.

Domsic, J.F., McKenna, R., 2010. Sequestration of carbon dioxide by the hydrophobic pocket of the carbonic anhydrases. Biochim. Biophys. Acta, Proteins Proteomics 1804 (2), 326–331.

Dunning, T.H., 1989. Gaussian basis sets for use in correlated molecular calculations. I. The atoms boron through neon and hydrogen. J. Chem. Phys. 90 (2), 1007–1023.

Floyd III, W.C., Baker, S.E., Valdez, C.A., Stolaroff, J.K., Bearinger, J.P., Satcher Jr, J.H., Aines, R.D., 2013. Evaluation of a carbonic anhydrase mimic for industrial carbon capture. Environ. Sci. Technol. 47 (17), 10049–10055.

Frisch, M.J., Trucks, G.W., Schlegel, H.B., Scuseria, G.E., Robb, M.A., Cheeseman, J.R., Scalmani, G., Barone, V., Mennucci, B., Petersson, G.A., Nakatsuji, H., Caricato, M., Li, X., Hratchian, H.P., Izmaylov, A.F., Bloino, J., Zheng, G., Sonnenberg, J.L., Hada, M., Ehara, M., Toyota, K., Fukuda, R., Hasegawa, J., Ishida, M., Nakajima, T., Honda, Y., Kitao, O., Nakai, H., Vreven, T., Montgomery, J.A., Peralta, J.E., Ogliaro, F., Bearpark, M., Heyd, J.J., Brothers, E., Kudin, K.N., Staroverov, V.N., Kobayashi, R., Normand, J., Raghavachari, K., Rendell, A., Burant, J.C., Iyengar, S.S., Tomasi, J., Cossi, M., Rega, N., Millam, J.M., Klene, M., Knox, J.E., Cross, J.B., Bakken, V., Adamo, C., Jaramillo, J., Gomperts, R., Stratmann, R.E., Yazyev, O., Austin, A.J., Cammi, R., Pomelli, C., Ochterski, J.W., Martin, R.L., Morokuma, K., Zakrzewski, V.G., Voth, G.A., Salvador, P., Dannenberg, J.J., Dapprich, S., Daniels, A.D., Farkas, Ö., Foresman, J.B., Ortiz, J.V., Cioslowski, J., Fox, D.J., 2009. Gaussian 09, Revision A.02. Gaussian, Inc, Wallingford CT.

Gómez-Díaz, D., Navaza, J.M., Sanjurjo, B., 2009. Mass-transfer enhancement or reduction by surfactant presence at a gas – liquid interface. Ind. Eng. Chem. Res. 48 (5), 2671–2677.

Guillet, G.L., Gordon, J.B., Di Francesco, G.N., Calkins, M.W., Cizmar, E., Abboud, K.A., Meisel, M.W., Garcia-Serres, R., Murray, L.J., 2015. A family of tri- and dimetallic pyridine dicarboxamide cryptates: unusual O,N,O-coordination and facile access to secondary coordination sphere hydrogen bonding interactions. Inorg. Chem. 54 (6), 2691–2704.

Gupta, R., Lacy, D.C., Bominaar, E.L., Borovik, A.S., Hendrich, M.P., 2012. Electron paramagnetic resonance and Mossbauer spectroscopy and density functional theory analysis of a high-spin Fe(IV)-oxo complex. J. Am. Chem. Soc. 134 (23), 9775–9784.

Huang, D., Makhlynets, O.V., Tan, L.L., Lee, S.C., Rybak-Akimova, E.V., Holm, R.H., 2011a. Kinetics and mechanistic analysis of an extremely rapid carbon dioxide fixation reaction. Proc. Natl. Acad. Sci. U. S. A. 108 (4), 1222–1227.

Huang, D., Makhlynets, O.V., Tan, L.L., Lee, S.C., Rybak-Akimova, E.V., Holm, R.H., 2011b. Fast carbon dioxide fixation by 2,6-pyridinedicarboxamidato-nickel(II)-hydroxide complexes: influence of changes in reactive site environment on reaction rates. Inorg. Chem. 50 (20), 10070–10081.

Huang, Q.Z., Thompson, J., Bhatnagar, S., Chandan, P., Remias, J.E., Selegue, J.P., Liu, K.L., 2014. Impact of flue gas contaminants on monoethanolamine thermal degradation. Ind. Eng. Chem. Res. 53 (2), 553–563.

Kelsey, R.A., Miller, D.A., Parkin, S.R., Liu, K., Remias, J.E., Yang, Y., Lightstone, F.C., Liu, K., Lippert, C.A., Odom, S.A., 2016. Carbonic anhydrase mimics for enhanced $CO_2$ absorption in an amine-based capture solvent. Dalton Trans. 45 (1), 324–333.

Kim, S., Saracini, C., Siegler, M.A., Drichko, N., Karlin, K.D., 2012. Coordination chemistry and reactivity of a cupric hydroperoxide species featuring a proximal H-bonding substituent. Inorg. Chem. 51 (23), 12603–12605.

Koziol, L., Valdez, C.A., Baker, S.E., Lau, E.Y., Floyd, W.C., Wong, S.E., Satcher, J.H., Lightstone, F.C., Aines, R.D., 2012. Toward a small molecule, biomimetic carbonic anhydrase model: theoretical and experimental investigations of a panel of zinc(II) aza-macrocyclic catalysts. Inorg. Chem. 51 (12), 6803–6812.

Koziol, L., Essiz, S.G., Wong, S.E., Lau, E.Y., Valdez, C.A., Satcher Jr, J.H., Aines, R.D., Lightstone, F.C., 2013. Computational analysis of a Zn-bound tris(imidazolyl) Calix [6]arene aqua complex: toward incorporating second-coordination sphere effects into carbonic anhydrase biomimetics. J. Chem. Theory Comput. 9 (3), 1320–1327.

Kyoto Protocol to the United Nations Framework Convention on Climate Change, Dec. 10, 1997, U.N. Doc FCCC/CP/1997/7/Add.1, 37 I.L.M. 22 (1998).

Lacy, D.C., Mukherjee, J., Lucas, R.L., Day, V.W., Borovik, A.S., 2013. Metal complexes with varying intramolecular hydrogen bonding networks. Polyhedron 52, 261–267.

Lau, E.Y., Wong, S.E., Baker, S.E., Bearinger, J.P., Koziol, L., Valdez, C.A., Satcher Jr, J.H., Aines, R.D., Lightstone, F.C., 2013. Comparison and analysis of zinc and cobalt-based systems as catalytic entities for the hydration of carbon dioxide. PLoS One 8 (6), e66187.

Liang, Z.W., Rongwong, W., Liu, H.L., Fu, K.Y., Gao, H.X., Cao, F., Zhang, R., Sema, T., Henni, A., Sumon, K., Nath, D., Gelowitz, D., Srisang, W., Saiwan, C., Benamor, A., Al-Marri, M., Shi, H.C., Supap, T., Chan, C., Zhou, Q., Abu-Zahra, M., Wilson, M., Olson, W., Idem, R., Tontiwachwuthikul, P., 2015. Recent progress and new developments in post-combustion carbon-capture technology with amine based solvents. Int. J. Greenhouse Gas Control 40, 26–54.

Lindskog, S., 1997. Structure and mechanism of carbonic anhydrase. Pharmacol. Ther. 74 (1), 1–20.

Lippert, C.A., Liu, K., Sarma, M., Parkin, S.R., Remias, J.E., Brandewie, C.M., Odom, S.A., Liu, K.L., 2014a. Improving carbon capture from power plant emissions with zinc- and cobalt-based catalysts. Catal. Sci. Technol. 4 (10), 3620–3625.

Lippert, C.A., Widger, L.R., Sarma, M., Liu, K.L., 2014b. Catalyst development for rate enhanced acid gas ($CO_2$) scrubbing. Energy Procedia 63, 273–278.

Mannel, D.S., Qi, G., Widger, L.R., Bryant, J., Liu, K., Fegenbush, A., Lippert, C.A., Liu, K., 2017. Enhancements in mass transfer for carbon capture solvents part II: micron-sized solid particles. Int. J. Greenhouse Gas Control 61, 138–145.

Nakata, K., Shimomura, N., Shiina, N., Izumi, M., Ichikawa, K., Shiro, M., 2002. Kinetic study of catalytic CO2 hydration by water-soluble model compound of carbonic anhydrase and anion inhibition effect on CO2 hydration. J. Inorg. Biochem. 89 (3–4), 255–266.

Paris Agreement, 2016. United Nations Treaty Collection. 8 July. .

Parkin, G., 2004. Synthetic analogues relevant to the structure and function of zinc enzymes. Chem. Rev. 104 (2), 699–768.

Parson, E.A., Keith, D.W., 1998. Science 282 (5391), 1053.

Rao, A.B., Rubin, E.S., Technical, A., 2002. Economic, and environmental assessment of amine-based $CO_2$ capture technology for power plant greenhouse gas control. Environ. Sci. Technol. 36 (20), 4467–4475.

Rogelj, J., den Elzen, M., Hohne, N., Fransen, T., Fekete, H., Winkler, H., Schaeffer, R., Sha, F., Riahi, K., Meinshausen, M., 2016. Paris Agreement climate proposals need a boost to keep warming well below 2 degrees C. Nature 534 (7609), 631–639.

Sahu, S., Widger, L.R., Quesne, M.G., de Visser, S.P., Matsumura, H., Moenne-Loccoz, P., Siegler, M.A., Goldberg, D.P., 2013. Secondary coordination sphere influence on the reactivity of nonheme iron(II) complexes: an experimental and DFT approach. J. Am. Chem. Soc. 135 (29), 10590–10593.

Sahu, S., Quesne, M.G., Davies, C.G., Durr, M., Ivanovic-Burmazovic, I., Siegler, M.A., Jameson, G.N., de Visser, S.P., Goldberg, D.P., 2014. Direct observation of a nonheme iron(IV)-oxo complex that mediates aromatic C-F hydroxylation. J. Am. Chem. Soc. 136 (39), 13542–13545.

Sahu, S., Zhang, B., Pollock, C.J., Durr, M., Davies, C.G., Confer, A.M., Ivanovic-Burmazovic, I., Siegler, M.A., Jameson, G.N., Krebs, C., Goldberg, D.P., 2016. Aromatic C-F hydroxylation by nonheme Iron(IV)-Oxo complexes: structural, spectroscopic, and mechanistic investigations. J. Am. Chem. Soc. 138 (39), 12791–12802.

Scalmani, G., Frisch, M.J., 2010. Continuous surface charge polarizable continuum models of solvation. I. General formalism. J. Chem. Phys. 132 (11), 114110.

Shook, R.L., Borovik, A.S., 2010a. The role of the secondary coordination sphere in metal-mediated dioxygen activation. Inorg. Chem. 49 (8), 3646–3660.

Shook, R.L., Borovik, A.S., 2010b. Role of the secondary coordination sphere in metal-mediated dioxygen activation. Inorg. Chem. 49 (8), 3646–3660.

Sivanesan, D., Youn, M.H., Murnandari, A., Kang, J.M., Park, K.T., Kim, H.J., Jeong, S.K., 2017. Enhanced $CO_2$ absorption and desorption in a tertiary amine medium with a carbonic anhydrase mimic. J. Ind. Eng. Chem. 52 (Supplement C), 287–294.

Soo, H.S., Komor, A.C., Iavarone, A.T., Chang, C.J., 2009. A hydrogen-bond facilitated cycle for oxygen reduction by an acid- and base-compatible iron platform. Inorg. Chem. 48 (21), 10024–10035.

Span, E.A., Suess, D.L.M., Deller, M.C., Britt, R.D., Marletta, M.A., 2017. The role of the secondary coordination sphere in a fungal polysaccharide monooxygenase. ACS Chem. Biol. 12 (4), 1095–1103.

Thompson, J.G., Frimpong, R., Remias, J.E., Neathery, J.K., Liu, K., 2014. Heat stable salt accumulation and solvent degradation in a pilot-scale CO2 capture process using coal combustion flue gas. Aerosol Air Qual. Res. 14 (2), 550–558.

Thompson, J.G., Bhatnagar, S., Combs, M., Abad, K., Onneweer, F., Pelgen, J., Link, D.,

Figueroa, J., Nikolic, H., Liu, K., 2017. Pilot testing of a heat integrated 0.7 MWe $CO_2$ capture system with two-stage air-stripping: amine degradation and metal accumulation. Int. J. Greenhouse Gas Control 64, 23–33.

Wada, A., Harata, M., Hasegawa, K., Jitsukawa, K., Masuda, H., Mukai, M., Kitagawa, T., Einaga, H., 1998. Structural and spectroscopic characterization of a mononuclear hydroperoxo–copper(II) complex with tripodal pyridylamine ligands. Angew. Chem., Int. Ed. 37 (6), 798–799.

Widger, L.R., Jiang, Y., McQuilken, A.C., Yang, T., Siegler, M.A., Matsumura, H., Moenne-Loccoz, P., Kumar, D., de Visser, S.P., Goldberg, D.P., 2014a. Thioether-ligated iron (II) and iron(III)-hydroperoxo/alkylperoxo complexes with an H-bond donor in the second coordination sphere. Dalton Trans. 43 (20), 7522–7532.

Widger, L.R., Davies, C.G., Yang, T., Siegler, M.A., Troeppner, O., Jameson, G.N., Ivanovic-Burmazovic, I., Goldberg, D.P., 2014b. Dramatically accelerated selective oxygen-atom transfer by a nonheme iron(IV)-oxo complex: tuning of the first and second coordination spheres. J. Am. Chem. Soc. 136 (7), 2699–2702.

Widger, L.R., Sarma, M., Bryant, J.J., Mannel, D.S., Thompson, J.G., Lippert, C.A., Liu, K., 2017. Enhancements in mass transfer for carbon capture solvents part I: homogeneous catalyst. Int. J. Greenhouse Gas Control 63, 249–259.

Zhang, X.P., Vaneldik, R., 1995. A functional model for carbonic anhydrase - thermodynamic and kinetic study of a tetraazacyclododecane complex of zinc(II). Inorg. Chem. 34 (22), 5606–5614.

Zhang, X.P., Vaneldik, R., Koike, T., Kimura, E., 1993. Kinetics and mechanism of the hydration of $CO_2$ and dehydration of $HCO_3^-$ catalyzed by a Zn(II) complex of 1,5,9-triazacyclododecane as a model for carbonic anhydrase. Inorg. Chem. 32 (25), 5749–5755.

Zhao, Y., Truhlar, D.G., 2008. The M06 suite of density functionals for main group thermochemistry, thermochemical kinetics, noncovalent interactions, excited states, and transition elements: two new functionals and systematic testing of four M06-class functionals and 12 other functionals. Theor. Chem. Acc. 120 (1), 215–241.